

## DEM GENERATION IN TAIWAN BY USING INSAR AND ERS DATA

Jaan-Rong TSAY<sup>1</sup> and Hung-Hsu Chen<sup>2</sup>

Assistant Professor<sup>1</sup> and graduate student<sup>2</sup>, Department of Surveying Engineering

National Cheng Kung University

1, University Road, 70101 Tainan

Tel: (886)-6-237-0876 ext. 838 Fax: (886)-6-237-5764

E-mail: tsayjr@mail.ncku.edu.tw

TAIWAN, R.O.C.

**KEY WORDS:** INSAR, DEM, Tandem mode, SLC, ERS

**ABSTRACT:** This paper analyzes the algorithm of SAR interferometry for generating a DEM in Taiwan. Our preliminary test results show that the DEM determined using INSAR and ERS data has an accuracy of about 23m in average in urban area, and about 5m in bare areas without vegetation and buildings, if all data in areas with usable radar echoes (higher coherences) is processed properly.

### 1. INTRODUCTION

Imaging radar can be considered a relatively new remote sensing system in comparison to aerial photogrammetry. Imaging radars are generally considered to include wavelengths from 1mm to 1m. Water clouds have a significant effect only on radars operating below 2cm in wavelength; the effects of rain are relatively inconsequential at wavelengths above 4cm. Radar is an active sensor, transmitting a signal of electromagnetic energy, illuminating the terrain, and recording or measuring the response returned from the target or surface. It can operate day or night. Both weather independence and 24-hour imaging capabilities are the two most notable or widely touted characteristics of radars (Henderson and Lewis, 1998). In this paper, we study some aspects on the generation of digital elevation model (DEM) in Taiwan using the SAR interferometry (INSAR) and ERS1/2 data.

### 2. ALGORITHM FOR DEM GENERATION BY SAR INTERFEROMETRY

Two subsystems of the Vexcel's 3DSAR SAR processing system package are used in our tests. They are FOCUS and PHASE. The computation procedures adopted in our tests and for our test data are described briefly as follows. For detail please see (Vexcel, 2000).

Firstly, FOCUS uses the raw SAR data (phase history data) in the CEOS L0 format to produce output data in the standard CEOS L1 format. This SAR processor – FOCUS – is already described briefly in (Tsay and Lu, 2001). Then, a digital elevation model (DEM) is generated as follows, where there are seven steps that must be completed for each pair of SLC (single-look complex) images.

1. **Estimate baseline:** an initial estimate of the baseline is determined so that one may decide whether further processing will be useful. It is not used in any subsequent processing.

2. **Register and resample the two SLC images:** this process calculates the mapping required to register the secondary SLC to the reference SLC and resamples the secondary SLC. To calculate the registration, a large number of tie points – points whose position in both images is known – and fit them to a linear function. Only the tie point with good quality, namely its SNR (Signal-to-Noise Ratio) is larger than a given threshold, is included in the fit. The RMS errors in the vertical and the horizontal directions respectively are divided by the square root of the number of tie points. Both numbers should be less than 0.03 pixels for a good registration. During resampling, the Fourier spectrum of the secondary SLC is filtered so that only the portion of the spectrum, which exactly overlaps the spectrum of the reference SLC, is retained. For large squint angles or large baselines, this spectral filtering can significantly improve the quality of the interferogram.

3. **Calculate interferogram:** the interferogram is calculated through a complex conjugate multiply of the reference SLC and the resampled secondary SLC, where the reference SLC is filtered so that only the overlapping spectral bandwidth is retained. Also, the baseline may be estimated either from the accurate satellite ephemeris data or directly from the registration coefficients, where satellite ephemeris contains the position and velocity of the satellite at a specific time. This process will provide the multi-looked power images for the reference SLC and the resampled

secondary SLC respectively, the coherence image, and the spherical earth phase as well. The spherical earth phase must be added to the phase in the interferogram to get the full interferometric phase. The coherence is a measure of the quality of the interferometric phase. It is a number between zero and one, one if the phase is perfectly accurate and zero if there is no accuracy.

4. **Filter interferogram:** the Goldstein filter (Goldstein and Werner, 1997) is used in our tests for filtering interferogram data. It takes 2D Fourier transforms of small patches of the interferogram and changes the spectrum  $s$  to the new spectrum  $s'$  by

$$s' = s|s|^{\mathbf{a}} \quad (1)$$

where the parameter  $\mathbf{a}$  can be set. The useful filter parameter values are  $\mathbf{a} = 0.0-2.0$ . The Goldstein filter is fast and very useful in scenes with rapid phase variations.

5. **Unwrap interferogram:** convert the image of (wrapped) phase values which are in the range of  $-\pi$  to  $\pi$  to a continuous (unwrapped) function. This is called *phase unwrapping*. PHASE provides two available unwrapping methods, the Goldstein method (Goldstein et al. 1988; Ghiglia and Pritt, 1998) and the Quality-Guided-Branch-Cuts (QGBC) method (Flynn, 1995; Ghiglia and Pritt, 1998). Both are path following unwrapping algorithms, which find all of the residues in the interferogram and connect the residues with branch cuts. The Goldstein method connects the residues with the shortest network of branch cuts possible and the QGBC method connects the residues with branch cuts that lie along the greatest phase uncertainty. The Goldstein method is usually much faster than QGBC, but there may be unwrapping errors in regions of large phase uncertainty. Unwrapping errors usually occur in regions of low coherence. It is suggested that the Goldstein method be used first, and then if there are significant unwrapping errors in the region of interest that the QGBC method be tried. A point with a high coherence may be selected as the starting pixel for both path-following unwrapping algorithms. Pixels with a value of coherence less than the coherence threshold will not be unwrapped. Useful values for the coherence threshold are in the range of 0.0 to 0.2.

6. **Refine geometry using GCPs:** a list of carefully selected ground control points (GCPs) is used to compute a corrected trajectory for the reference satellite pass (the satellite ephemeris) and to correct the baseline between two passes. Refining the satellite ephemeris is required for accurate ortho-rectification of output products, refining the baseline is needed to determine accurate elevation values. With a source of auxiliary data, such as a topographic map and the reference power image, the image position  $(x,y)$  can be tied to a map position  $(X,Y,Z)$ . The quality of the determined DEM will depend both on the accuracy of the GCPs selected and their number. In general, at least 10 GCPs should be collected. The more the GCPs used, the more accurate the DEM determined using INSAR.

7. **Create height map:** this process output an ortho-rectified DEM and an ortho-rectified SAR image. The vertical and horizontal datums for the height map can be chosen. In addition, the pixel spacing can be set in both the  $X$  and the  $Y$  direction. A program to change the height map data to a DEM in ASCII format  $(X,Y,Z)$  is developed by ourselves to enable our quality analysis on the determined DEM.

### 3. TEST RESULTS

In comparison to the Cband data of ERS1/2 and RADARSAT, JERS data is less susceptible to temporal decorrelation because of its lower L-band frequency. In other words, JERS data is ideal for repeat-pass spaceborne interferometry. Nevertheless, the ERS data is adopted in our tests since no JERS data is available to us for the present. More clearly to say, the Tandem mode data is used in our tests. They are ① ERS1 in the raw CEOS format from the track 461 and the orbit 22994 taken on December 8, 1995, and ② ERS2 in the raw CEOS format from the track 461 and the orbit 3321 taken on December 9, 1995. The perpendicular and parallel baselines are approximately 205m and 78m, respectively. For good results, the perpendicular baseline should be between 25m and 300m for ERS data (Vexel, 2000). If the baseline is too small, there will be no sensitivity to topography. If the baseline is too large, the phase data will be corrupted by baseline decorrelation. Figure 1 shows the power image of the reference SLC (ERS2, 1995/12/09) and the multi-looked image in the test area.

The registration results show that the errors of the fit in the azimuth and range directions are 0.14 and 0.09 pixels, respectively. 550 tie points were used to compute the fit by an Affine transform relating the secondary SLC (ERS1, 1995/12/08) and the reference SLC (ERS2, 1995/12/09). In order to generate a good interferogram, the errors must be less than one pixel and the number of tie points should be large (greater than 100). If the fit is not good, or if the number of tie points is too small, the SNR threshold should be changed. Decreasing the SNR threshold will result in more tie points. Increasing the SNR threshold will reduce the number of tie points but the remaining ones will be more

accurate.

When PHASE resamples the secondary SLC, it filters both the range (horizontal) and along-track (vertical) spectrum so that, when the interferogram is created, maximum coherence is obtained. In our test pair, the range and along-track spectrum is filtered so that only 58% and 60% of the bandwidth is retained, respectively. If the retained portion of the either range or along-track bandwidth falls below 50%, the pair may not make a good interferogram. The amount of retained along-track and range bandwidth depends on the difference in the Doppler frequencies of the two acquisitions and the baseline, respectively. If the Doppler frequencies of the two acquisitions are different, too little along-track bandwidth is retained. If the baseline is too large, too little range bandwidth is retained. The interferogram is generated using two range looks and ten azimuthal looks. Figure 2 shows the coherence image and the interferogram. In the coherence image, low values of coherence are blue, higher coherence is magenta and then yellow, and the highest coherence is green. The coherence value in the coherence image is the magnitude of the interferogram smoothed over a 3x3 window. When the generation of the interferogram is completed, the baseline is estimated again. The baseline estimated in this step is superior to the one computed in the previous “Estimate Baseline” process, since the registration information is utilized in this step to aid the calculation.

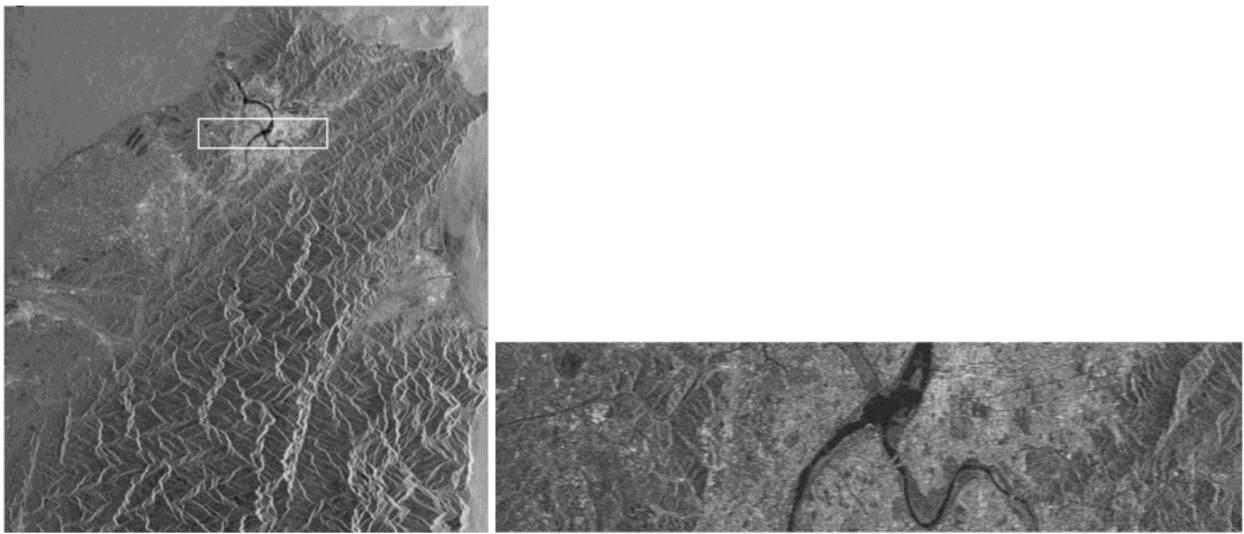


Figure 1. Power image of the reference SLC (left), where the rectangle shows the test area, and the multi-looked image in the test area (right).

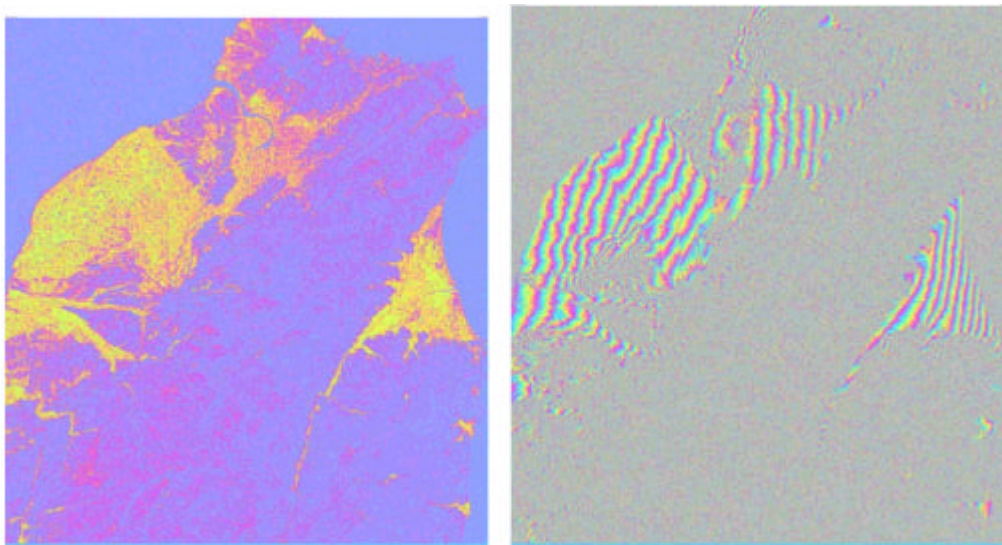


Figure 2. Coherence image (left) and the interferogram (right).

Figure 2 shows apparently that high coherence occurs in urban areas. The mountain regions has low coherence. The ocean areas have a coherence of zero. Moreover, the higher the coherence, the clearer the interferometric fringes.

Before unwrapping the phase, the interferogram is firstly smoothed to remove some of the phase noise. This will make

unwrapping easier. The Goldstein filter with the default value  $\alpha=1$  is used because this process will finish quickly. The thus filtered interferogram is shown in Figure 3. Comparing to the Figure 2 (right) shows that the filtered phase is much more smooth than the original interferometric phase.

Now, the Goldstein method is used to unwrap the phase, where the coherence threshold is set to 0.1. This will prevent unwrapping into regions where the coherence is smaller than 0.1, such as the ocean and mountainous areas. A seed point that has good phase data all round is chosen and the unwrapping starts from this seed point. Test results show that the unwrapped phase looks almost the same as the filtered interferogram except that there are some holes that were not unwrapped because the coherence was below the coherence threshold. On the left in Figure 4, the unwrapped phase image in the test area is shown. Because the seed pixel is located in the test area (urban area in the north Taiwan) and this area has very low coherence all around, the unwrapped phase image covers merely the test area, a northern portion of the entire interferogram shown in Figures 2 and 3.

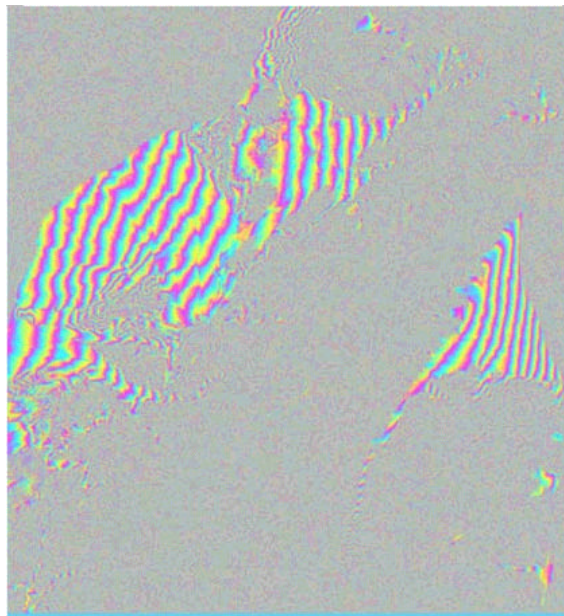


Figure 3. Filtered interferogram using the Goldstein filter with  $\alpha=1$ .

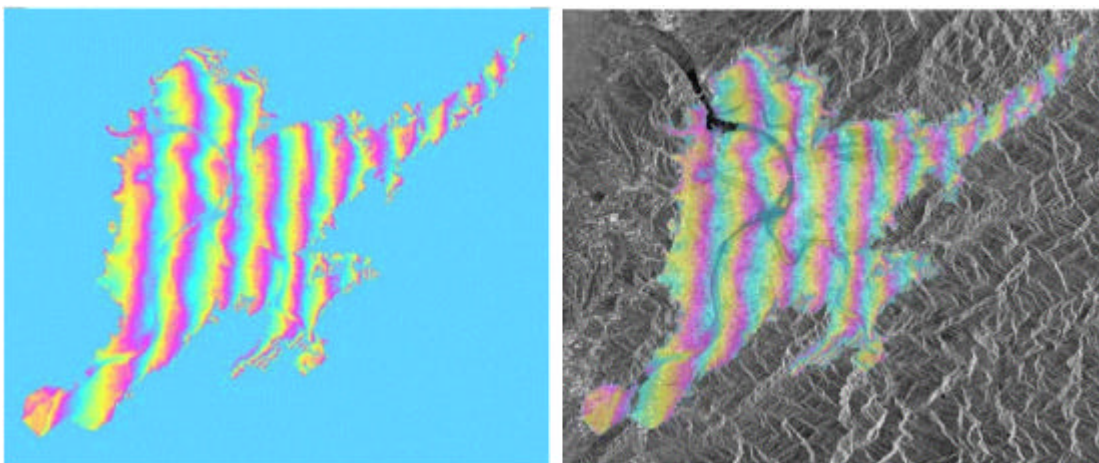


Figure 4. Unwrapped phase (left) and the unwrapped phase image overlaid with the power image (right) in the test area.

Before generating the DEM, 84 GCPs are used to refine the baseline estimated in the previous “Calculate Interferogram” process, and to find an additive constant with which the unwrapped phase is to be corrected. Usually 12 to 20 GCPs are sufficient. Their values  $X, Y$  are used to refine the satellite ephemeris, which is used to ortho-rectify output products. These values should have an accuracy of a few tens of meters or better unless refining the ephemeris is disabled.

We use the ortho image of the scale 1/10000 and the DEM with a grid size of 5m x 5m in the test area. Both are

generated using aerial images with an average scale of 1/5000. The flight height is about 1600m above the ground. All aerial photos are taken between October 1997 and January 2000, about 2-4 years later when our Tandem mode data were acquired (December 8-9, 1995). Since no other better data is available, GCPs are extracted from them. It is assumed that no significant ground surface deformation occurred during that time. The locations of all 84 GCPs are shown on the left in Figure 5. It shows apparently that the eastern portion in test area don't have any GCP.

To generate the DEM, the projection is set to UTM and the horizontal and vertical datums are set to WGS84. Before utilizing all GCPs data, they are transformed from their original coordinate system - Taiwan Datum 1997 (TWD97) – to the WGS84. The DEM is calculated using those 84 GCPs. The height map is shown on the right in Figure 5.

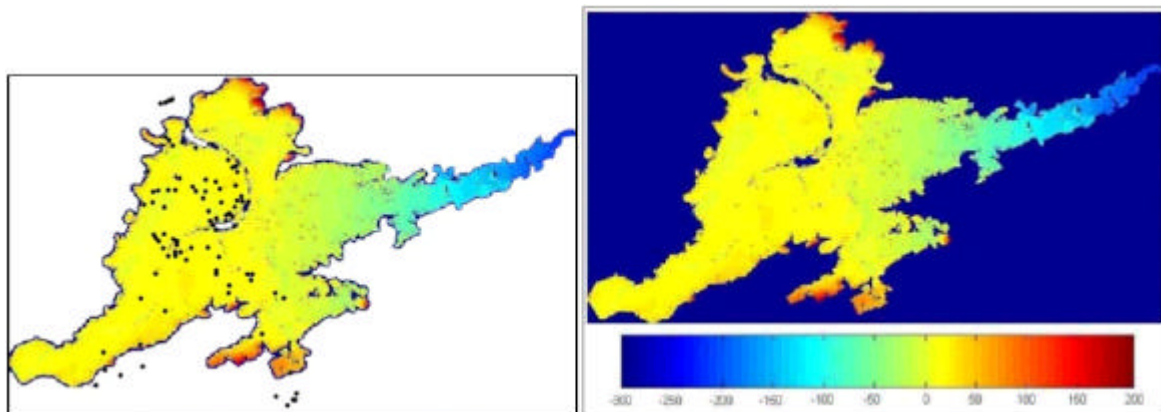


Figure 5. Locations of all 84 GCPs (left) and the determined height map (right).

The height map shows apparently that the DEM data in its eastern mountainous area is wrong, since they should not have height values less than 0m. This area is mountainous and covered with dense vegetation. It appears a difficult area for spaceborne INSAR to calculate the DEM. The 5m x 5m DEM determined using aerial photogrammetry only covers the area shown on the right in Figure 7. In this area, there are altogether 93850 common height points. They show that the mean height difference between the DEM determined by aerial photogrammetry, denoted by  $H_{AP}$ , and the one determined by INSAR, denoted by  $H_{SAR}$ , is  $-3.70\text{m}$  with  $dH = H_{SAR} - H_{AP}$ . Their root mean square (RMS) value is about 23m. Figure 6 shows their histogram and distribution map in the test area.

Among them, 86% of those common height points has  $|dH| \leq 20\text{m}$ . These points are almost located in the urban area. Figure 7 shows their distribution map and the ortho aerial image in test area. Both  $dH$ -distribution map and the ortho image in the same area show clearly that almost all height points with  $|dH| \leq 5\text{m}$  lie in the near bare regions without dense vegetation and buildings. The other points with  $5\text{m} < |dH| \leq 20\text{m}$  lie apparently in the regions with dense high buildings. The 3D  $dH$ -surface looks like a rough 3D city model in these area.

On the other hand, comparing the height map shown in Figure 5 with the ortho image shown in Figure 7 shows that spaceborne INSAR also calculates the height values over the shallows in rivers and with high buildings around. They may be caused by multi-scattering effect of radar echoes in these areas. Of course, this effect may cause errors in the DEM determined.

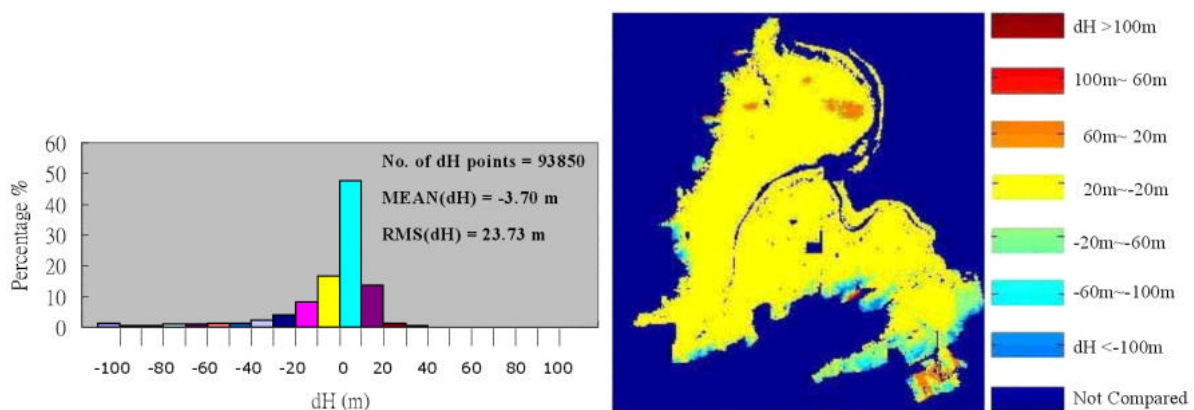


Figure 6. Histogram (left) and distribution map of  $dH = H_{SAR} - H_{AP}$  in test area (right).

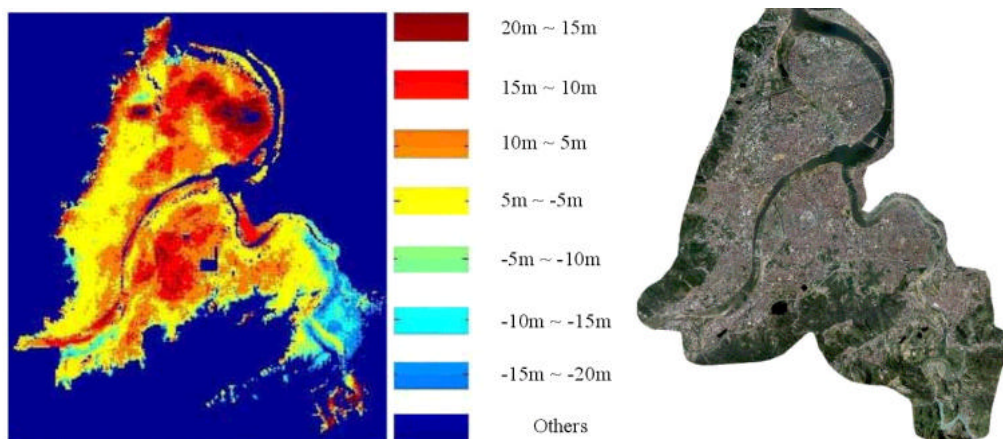


Figure 7. Distribution map of dH with  $|dH| \leq 20m$  (left) and the ortho aerial image in test area (right).

#### 4. CONCLUSIONS

It is well-known that Taiwan is an island in subtropical zone on the earth. Our preliminary test results show that the DEM determined using INSAR and ERS data has in average an accuracy of about 23m in urban area, and about 5m in bare areas without vegetation and buildings, if all data in areas with usable radar echoes (higher coherences) is processed properly.

Mountainous areas with dense vegetation in Taiwan are still difficult areas for the digital elevation model (DEM) generation using the spaceborne INSAR technique and ERS data in Tandem mode. It needs more studies and tests to find an applicable solution for generating precise DEM in those difficult areas. We intend to study directly the airborne INSAR in the coming years, because our main interests aim at determining a high accurate DEM in those difficult areas for aerial photogrammetry.

#### 5. REFERENCES

- Flynn, T.J., 1995. Consistent 2-D phase unwrapping guided by a quality map, Proceedings of the 1996 International Geoscience and Remote Sensing Symposium, Lincoln, NE, May27-31, IEEE, Piscataway, NJ, p2057.
- Ghiglia, D.C., and Pritt, M.C., 1998. Two Dimensional Phase Unwrapping, John Wiley & Sons, New York, p103, p136.
- Goldstein, R., and Werner, C., 1997. Radar Ice Motion Interferometry. 3rd ERS Symposium, Florence Italy.
- Goldstein, R.M., Zebker, H.A., and Werner, C.L., 1988. Satellite radar interferometry: two-dimensional phase unwrapping, Radio Science, Vol. 23, No. 4, p713.
- Henderson, F.M., and Lewis, A.J., 1998. Principles and Applications of Imaging Radar. John Wiley & Sons, New York, pp. 2-4.
- Tsay, J.-R., and Lu, C.-H., 2001. Quality Analysis on Height Displacement Values Determined by Three-Pass Method and some Test results in Urban Area in Taiwan. To be presented in ACRS2001 (paper no. 103).
- Vexcel, 2000. 3dSAR SAR Processing System, User's Manual.